

Multifractal characterization of cerebrovascular dynamics in newborn rats

A.N. Pavlov^{a,b,*}, O.V. Semyachkina-Glushkovskaya^c, V.V. Lychagov^a,
A.S. Abdurashitov^a, O.N. Pavlova^a, O.A. Sindeeva^c, S.S. Sindeev^c

^a Department of Physics, Saratov State University, Astrakhanskaya Str. 83, Saratov, 410012, Russia

^b Saratov State Technical University, Politehnicheskaya Str. 77, Saratov, 410054, Russia

^c Department of Biology, Saratov State University, Astrakhanskaya Str. 83, Saratov, 410012, Russia

ARTICLE INFO

Article history:

Received 22 February 2015

Accepted 13 April 2015

ABSTRACT

In this paper we study the cerebrovascular dynamics in newborn rats using the wavelet-based multifractal formalism in order to reveal effective markers of early pathological changes in the macro- and microcirculation at the hidden stage of the development of intracranial hemorrhage (ICH). We demonstrate that the singularity spectrum estimated with the wavelet-transform modulus maxima (WTMM) technique allows clear characterization of a reduced complexity of blood flow dynamics and changes of the correlation properties at the transformation of normal physiological processes into pathological dynamics that are essentially different at the level of large and small blood vessels.

© 2015 Elsevier Ltd. All rights reserved.

1. Introduction

Multiscale phenomena in the dynamics of nonlinear systems are the subject of many studies performed during the last decades. Their characterization in natural sciences, as in physiology or earth science, is complicated by the non-stationarity of available experimental data. Additional difficulties in numerical analysis can be caused by a short duration of acquired time series and the presence of noise. These circumstances reduce possibilities of the standard data processing tools such as, spectral or correlation analysis. One of the most powerful approaches for statistical analysis of nonstationary and inhomogeneous processes is the wavelet-based multifractal formalism [1–3] that has demonstrated its essential potential in solving many applied problems [4–10]. Thus, application of this tool in physiology allowed proposing useful diagnostics measures that outperform abilities of

the standard techniques for data processing [11–13]. When characterising adaptation mechanisms in the cardiovascular dynamics with the multifractal formalism, distinct stress-induced responses are revealed being not distinguished with the spectral analysis [14,15]. Besides, characteristics of the WTMM-method demonstrate a quite fast convergence with the amount of data points as compared with the scaling exponent describing the decay of the correlation function, and the latter circumstance is important when dealing with short data series [15].

In this work we use the WTMM-approach for quantifying stress-induced changes in the cerebral blood flow (BF) in newborn rats leading to the development of ICH. This is an actual problem in neonatal medicine since the ICH represents one of the main reasons of mortality and morbidity in newborns. Its development typically occurs asymptomatic, and the corresponding mechanisms are still poorly understood [16]. Markers of early stages of the ICH development should be based on noninvasive analysis of impairments in the cerebral BF that can be done with optical imaging techniques such as, the laser speckle contrast imaging (LSCI) [17,18] that is widely used in medicine. LSCI provides

* Corresponding author at: Department of Physics, Saratov State University, Astrakhanskaya Str. 83, 410012 Saratov, Russia. Tel: +78 452 210710.
E-mail address: pavlov.lesha@gmail.com (A.N. Pavlov).

a high spatio-temporal resolution giving an opportunity to visualize the structure of blood vessels and to analyze dynamical changes of the BF velocity. A feature of studies performed in newborns is the requirement of revealing risk factors using quite short recordings of the BF velocity at the condition of nonstationarity. Besides the intrinsic dynamics of cerebral vessels, this nonstationarity can be caused by the head's moving, respiration, etc. Under these circumstances, the WTMM-approach could provide informative characterization of the hidden stage of the ICH development. In this paper we show that the stress-induced changes in the BF dynamics are different in small and large cerebral vessels. We discuss informative markers of pathological dynamics based on the multifractal characteristics of the BF velocity.

The paper is organized as follows. In Section 2, we describe experimental procedures and the WTMM-method used for data processing. In Section 3, we consider markers of early pathological changes in the cerebral BF caused by a severe stress and show that these markers allow quantification of impairments in the BF dynamics that occur during the hidden stage of the ICH development. Some concluding remarks are given in Section 4.

2. Experiments and methods

2.1. Experimental procedure

Experiments were carried out in 57 newborn male rats (2–3 days old). All procedures were performed in accordance with the Guide for the Care and Use of Laboratory Animals published by the US National Institute of Health (NIH Publication No. 85-23, revised 1996). The experimental protocols were approved by the Committee for the Care and Use of Laboratory Animals at Saratov State University (Saratov, Russia). The rats were housed at 25 ± 2 °C, 55% humidity, and 12:12 h light/dark cycle. To induce the development of ICH in newborn animals, a severe stress was applied. As a model of stress, we used an intermittent infrasound off) [19,20]. This procedure was performed in the Plexiglas chamber (the volume – 2000 cm³) amplifying deleterious effects of infrasound on rats. As it was shown in [21], the stress-induced ICH occurs during the next day after the stress. Here, we consider three groups of rats: a control group ($n=18$), a group with a latent (hidden) stage of the ICH development (4 h after the stress, $n=16$), and a group with the developed ICH (24 h after the stress, $n=23$).

The velocity of the cerebral BF was measured with the LSCI-technique through the fontanel in anesthetized rats (isoflurane – inhalant anesthetic) with the fixed head. Raw speckle images were recorded during 5 min at average rate of 40 frames/second. The images were preprocessed using an algorithm for the spatial contrast analysis that performs averaging within a moving window (55×55 pixels) over 50 speckle images. Temporal dynamics of BF was extracted from two regions: the sagittal sinus reflecting the macroscopic cerebral dynamics (macrocirculation), and small vessels (microcirculation). Thus, two time series of the BF velocity were acquired for each newborn rat.

2.2. Data analysis

The wavelet transform modulus maxima method is a commonly used technique to reveal multiscale phenomena

in nonstationary and inhomogeneous processes. Unlike the approach based on the structure functions [22], the WTMM-method provides an ability to quantify a wide range of scales associated with both, weak and strong singularities. A feature of characteristics estimated with the wavelet-based multifractal formalism (the spectrum of the Hölder exponents and the singularity spectrum [1,2]) is that they do not depend on the selected basic wavelet according to the theoretical background of the considered method. In practice, however, such a dependence appears, mainly due to short duration of data series.

Algorithmically, the WTMM-method consists of two stages. At the first stage, the wavelet transform of an analyzed signal $x(t)$ is estimated as follows:

$$W(a, b) = \frac{1}{a} \int_{-\infty}^{\infty} x(t) \psi \left(\frac{t-b}{a} \right) dt, \quad (1)$$

where $W(a, b)$ are the wavelet coefficients, a and b characterize the scale and the translation of the basic function ψ along the time axis. As the basic function ψ one typically uses wavelets constructed by differentiation of the Gaussian function

$$\psi^{(m)}(\theta) = (-1)^m \frac{d^m}{d\theta^m} \left[\exp \left(-\frac{\theta^2}{2} \right) \right] \quad (2)$$

with WAVE ($m=1$) and MHAT ($m=2$) wavelets representing the most popular variants of ψ . After performing the wavelet transform (1), the skeleton is extracted being the lines of the local minima and maxima of the wavelet transform $W(a, b)$ detected at each fixed scale a . The extracted skeleton contains all necessary information about singularities of the analyzed signal $x(t)$.

At the second stage, the partition functions $Z(q, a)$ are constructed

$$Z(q, a) = \sum_{l \in L(a)} |W(a, b_l(a))|^q, \quad (3)$$

where $L(a)$ is the set of all lines in skeleton observed at the scale a , $b_l(a)$ determines the position of the extreme value of $W(a, b)$ associated with the line l . By selecting the parameter q it becomes possible to “illuminate” features of the analyzed signal at different scales. The partition functions (3) demonstrate the following power-law dependence:

$$Z(q, a) \sim a^{\tau(q)}. \quad (4)$$

with $\tau(q)$ called as the scaling exponents. Their knowledge allows estimating the Hölder exponents

$$h(q) = \frac{d\tau(q)}{dq} \quad (5)$$

and the singularity spectrum

$$D(h) = qh - \tau(q). \quad (6)$$

The WTMM approach is significantly more stable than a local estimating of $h(q)$ from time series [2,3].

The spectrum of Hölder exponents $h(q)$ characterizes the presence of a correlated ($h > 0.5$), an anti-correlated ($h < 0.5$), and an uncorrelated ($h=0.5$) dynamics. Larger exponents $h(q)$ quantify a “smoother” time dependence $x(t)$. The Hölder exponent $h(0)$ typically takes the value similar to scaling exponent of the detrended fluctuation analysis [23]. However, the

latter technique is less appropriate for characterising multi-scale structure of time series.

Although the power-law dependence of the partition functions $Z(q, a)$ versus the scale a is valid in a wide range of scales, too short and too long lines of the skeleton may reduce the precision of estimating the scaling exponents $\tau(q)$. Due to this, we used the range $a \in [0.7; 4.0]$.

3. Results and discussion

The performed analysis has revealed essential distinctions between the stress-induced impairments in the BF dynamics related to macro- and microcirculation. Former studies [19,20] were concentrated on the macroscopic level of the sagittal sinus in order to characterize the development of the venous insufficiency. For this purpose, quite simple characteristics were considered, namely, the diameter of the vessel and the mean velocity of BF. A more thorough analysis of blood circulation in large and small veins based on advanced data processing tools could provide a new insight into the mechanisms responsible for the transition from normal to pathological vascular dynamics. Let us address this problem with the wavelet-based multifractal formalism. The WTMM approach provides informative characterization of the correlation properties and the multiscale structure of experimental data based on the scaling exponents $\tau(q)$, the Hölder exponents $h(q)$ and the singularity spectrum $D(h)$. In order to characterize main features of the singularity spectrum, estimations of two quantities are performed. The first quantity is the value of the Hölder exponent related to the maximum of $D(h)$, i.e. the Hölder exponent $h(0)$ associated with the most frequently observed singularity. It describes correlation properties of the analyzed data series and distinguishes between power-law anti-correlations ($0 < h < 0.5$), power-law correlations ($0.5 < h < 1$) and a “smoother” correlated behavior that may be different from the power-law dependence ($h > 1$). The second quantity is the width of the singularity spectrum Δ_h that can serve as a complexity measure describing distinctions from the simplest (the monofractal) behavior characterized by only one Hölder exponent and the singularity spectrum consisting of a single point. Larger Δ_h imply that the analyzed dynamical regimes become more complicated and require larger sets of the Hölder exponents for describing their multiscale properties.

The considered measures provide informative characterization of stress-induced changes in the cerebral BF in newborn rats. At the macroscopic level of the sagittal vein, a rat with the stress-induced latent stage of the ICH development demonstrates a reduced complexity of the BF dynamics (a narrower singularity spectrum) as compared with a normal animal. This reduced complexity can be treated as a sign of pathological changes in the normal physiological regulation of BF. Let us note that changes of the complexity are not accompanied by a shift of the singularity spectrum. The maxima of $D(h)$ nearly coincide before and after the stress. The value $h(0)$ is close to 1, i.e., to statistical properties of $1/f$ -noise that is typical for the normal physiological regulation in the cardiovascular system.

Another type of the stress-induced changes in the BF dynamics occurs at the microscopic level of small veins (Fig. 2). Unlike the sagittal vein, small vessels demonstrate a quite

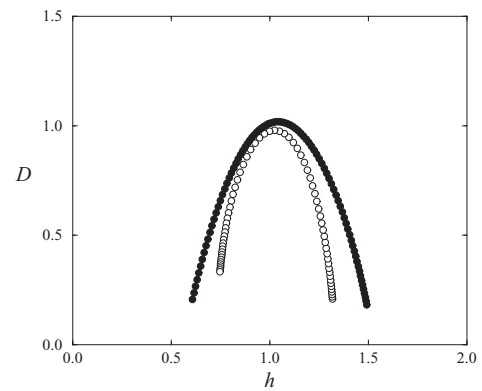


Fig. 1. Singularity spectra characterising the typical stress-induced changes in the macrocirculation (filled circles – control, open circles – 4 h after the stress).

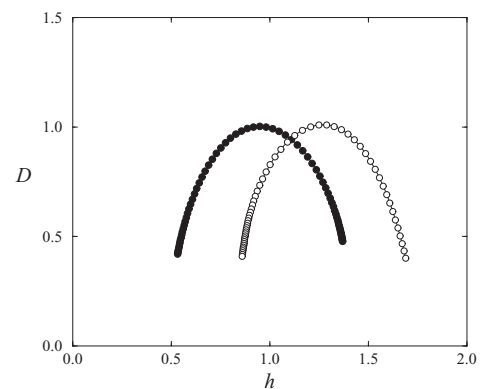


Fig. 2. Singularity spectra characterising the typical stress-induced changes in the microcirculation (filled circles – control, open circles – 4 h after the stress).

different response to severe stresses. Here, a shift of the singularity spectrum in the region of larger Hölder exponents is the main distinction between the BF dynamics before and after the stress. An increase of $h(q)$ represents an additional sign of pathological changes in the cardiovascular dynamics. For small vessels, a shift of the value $h(0)$ is a more informative marker of pathological changes in the BF regulation. Unlike the macrocirculation, the width of the singularity spectrum is slightly changed and, therefore, the complexity measure Δ_h is less appropriate for quantifying the development of ICH in newborn animals. Thus, according to the presented results, two markers are useful for describing the transformation of a normal physiological dynamics of cerebral vessels into a pathological dynamics: the Hölder exponent $h(0)$ at the microscopic level of small veins, and the width of the singularity spectrum Δ_h at the macroscopic level of the sagittal vein.

Figs. 1 and 2 illustrated the clearest stress-induced changes in the cerebral circulation. In practice, both the discussed effects (changes of the multifractality degree and the correlation properties) can be observed simultaneously, however, their impact at microscopic and macroscopic levels remains different that is illustrated by statistical analysis given in Fig. 3. According to Fig. 3a, the macroscopic cerebral dynamics in rats with the developed ICH (24 h after the stress)

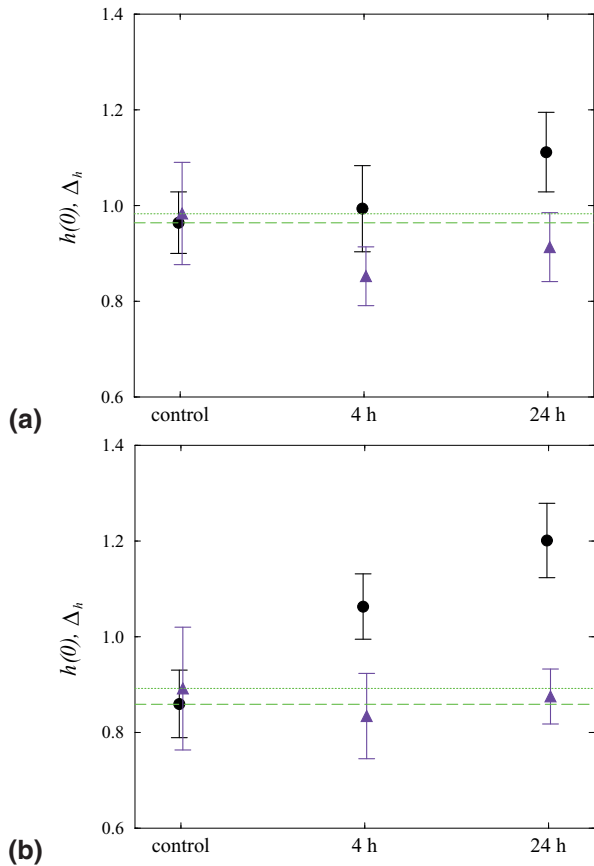


Fig. 3. Changes of multifractal characteristics at the level of large (a) and small (b) cerebral vessels. The results are shown as mean values \pm SE.

is characterized by significantly different values of $h(0)$ and Δ_h as compared with the control group: $h(0)=1.11 \pm 0.08$ vs. $h(0)=0.96 \pm 0.06$, $\Delta_h=0.91 \pm 0.07$ vs. $\Delta_h=0.98 \pm 0.11$. Therefore, we can conclude that pathological changes in the BF regulation include both, changes of the correlation properties and a reduced complexity of BF dynamics. However, at the hidden stage of the ICH development (4 h after the stress) only the second effect can clearly be diagnosed. Moreover, it is more pronounced as compared with the next day after the stress: $\Delta_h=0.85 \pm 0.06$ vs. $\Delta_h=0.91 \pm 0.07$.

At the microscopic level of small vessels, animals with the developed ICH demonstrate only a significant change of correlation properties of the BF dynamics without essential variations of the multiscality degree: $h(0)=1.20 \pm 0.08$ vs. $h(0)=0.86 \pm 0.07$, $\Delta_h=0.88 \pm 0.06$ vs. $\Delta_h=0.89 \pm 0.13$ (Fig. 3b). At the transient stage, the value Δ_h is slightly reduced ($\Delta_h=0.83 \pm 0.09$), however, these changes are small as compared with the macroscopic dynamics. Nevertheless, the observed shift of the singularity spectrum is well pronounced. Although the strongest distinctions are observed during the next day after the stress, analysis of the latent stage of the ICH development allows clear diagnostics of the stress-induced impairments in the cerebral microcirculation: $h(0)=1.06 \pm 0.07$ vs. $h(0)=0.86 \pm 0.07$. Changes of the correlation properties at the microscopic level of small veins outperform the corresponding changes at the macroscopic

level of the sagittal vein. Thus, simultaneous analysis of both, micro- and macrocirculation provides a way to diagnose the hidden stage of the ICH development. Because the observed effects are quite different, analysis of BF dynamics at the microscopic level could verify signs of a high risk of the ICH development revealed at the macroscopic level.

4. Conclusions

Characterization of the hidden stage of the ICH development is an important problem in neonatal medicine. Its detection with the standard physiological tools is generally ineffective because of the absence of clear symptoms. Due to this, new diagnostic markers based on non-invasive experimental techniques and advanced data processing tools are of a high importance. In this paper, we performed analysis of the cerebrovascular dynamics in newborn rats using the laser speckle contrast imaging being the optical interference technique that provides a way of studying vessels dynamics with high spatio-temporal resolution. Unlike previous studies in this field [19,20], we compared changes of macro- and microcirculation in animals during the development of ICH.

Data processing was performed with the WTMM-approach that allows statistical analysis of nonstationary and inhomogeneous processes and has demonstrated its potential in quantifying dynamics of complex systems from short and noisy data. We used two measures introduced based on the singularity spectrum: the Hölder exponent $h(0)$ related to the maximum of $D(h)$, and the width of the singularity spectrum that reflect correlation properties and complexity of the analyzed dynamics, respectively.

Based on these measures, we revealed essential distinctions between stress-induced impairments of cerebral macro- and microcirculation. At the level of large veins, the development of ICH is accompanied by a reduced complexity of BF dynamics described by a narrower singularity spectrum $D(h)$ without clear changes of the correlation properties. At the level of small veins, a shift of the singularity spectrum in the region of larger Hölder exponents appears that can be interpreted as an increased “smoothing” of experimental data. Both effects are clearly observed during the hidden stage and can be used for early diagnostics of pathological changes in the cerebral dynamics at the development of ICH.

Acknowledgments

This work has been supported by SFB-910 and the Russian Foundation for Basic Research (grant 14-52-12002). A.P. acknowledges support from the Ministry of Education and Science of Russian Federation in the framework of the implementation of state assignment 3.23.2014/K (project SSTU-157) and within the basic part (project SSTU-141). O.S.-G. acknowledges support from the President program for young scientists (MD-2216.2014.4) and the Russian Foundation for Basic Research (grant 14-02-00526a).

References

- [1] Muzy JF, Bacry E, Arneodo A. *Phys Rev Lett* 1991;67:3515.
- [2] Muzy JF, Bacry E, Arneodo A. *Phys Rev E* 1993;47:875.
- [3] Muzy JF, Bacry E, Arneodo A. *Int J Bifurcat Chaos* 1994;4:245.
- [4] Nunes Amaral LA, et al. *Phys Rev Lett* 2001;86:6026.

- [5] Arneodo A, et al. *Physica A* 1998;249:439.
- [6] Arrault J, et al. *Phys Rev Lett* 1997;79:75.
- [7] Arneodo A, Decoster N, Roux SG. *Phys Rev Lett* 1999;83:1255.
- [8] Silchenko A, Hu C-K. *Phys Rev E* 2001;63:041105.
- [9] Ivanova K, Ausloos M. *Physica A* 1999;274:349.
- [10] Pavlov AN, et al. *Physica A* 2002;316:233.
- [11] Ivanov PCh, et al. *Nature* 1999;399:461.
- [12] Ivanov PCh, et al. *Chaos* 2001;11:641.
- [13] Stanley HE, et al. *Physica A* 1999;270:309.
- [14] Pavlov AN, Ziganshin AR, Klimova OA. *Chaos, Solitons and Fractals* 2005;24:57.
- [15] Pavlov AN, Anishchenko VS. *Physics-Uspokhi* 2007;50:819.
- [16] Ballabh P. *Pediatr Res* 2010;67:1.
- [17] Briers JD, Webster S. *J Biomed Opt* 1996;1:174.
- [18] Boas DA, Dunn AK. *J Biomed Opt* 2010;15:011109.
- [19] Semyachkina-Glushkovskaya OV, et al. *J Photon Lasers Med* 2013; 2:109.
- [20] Semyachkina-Glushkovskaya OV, et al. *J Innov Opt Health Sci* 2013; 6:1350023.
- [21] Thorburn RJ, et al. *Early Human Dev* 1982;7:221.
- [22] Frish U, Parisi G, Parisi G. *Turbulence and predictability in geophysical fluid dynamics and climate dynamics*. Amsterdam: North-Holland; 1985. p. 71.
- [23] Peng C-K, et al. *Chaos* 1995;5:82.